Near Surface Geophysics, 2010, **8**, 65-74 doi:10.3997/1873-0604.2009052

Application of electrical resistivity tomography to the environmental characterization of abandoned massive sulphide mine ponds (Iberian Pyrite Belt, SW Spain)

D. Gómez-Ortiz*, S. Martín-Velázquez, T. Martín-Crespo,
C. De Ignacio-San José and J. Lillo

Department of Biology and Geology, ESCET, Universidad Rey Juan Carlos, Edificio Departamental 2, despacho 260, C/Tulipán s/n, 28933 Móstoles, Madrid, Spain

Received October 2008, revision accepted September 2009

ABSTRACT

Mining activity in the Iberian Pyrite Belt, on the south-west of the Iberian Peninsula, has generated a great amount of mine tailing ponds, which once the extractive activity is finished, are abandoned and become a serious environmental problem. Here we present the results of applying the electrical resistivity tomography (ERT) technique to characterize the abandoned mine ponds in two sites: Monte Romero and Mina Concepción. ERT has allowed us to determine both the general geometry of the pond's base and the maximum thickness of the mine tailings. In all cases, the resistivity contrast between the infilling and the bedrock is high enough to clearly define the bottom pond boundary. The low-resistivity values (lower than 5 Ωm) obtained for the infilling are explained by the high concentration of pyrite in the tailings and the occurrence of acid waters. Whereas the Monte Romero mine pond is almost completely saturated with water, in Mina Concepción it has been possible to identify the presence of inner acid water flows, the outlet of which through the damaged dyke originates a spilling of acid waters to the Odiel River. No low-resistivity water flows through the base of the ponds into the bedrock have been observed, indicating a good isolation of the base of the studied mine ponds.

INTRODUCTION

The mining of copper from sulphide ores, in addition to metal production, generates large amounts of mine tailings that are deposited in mine ponds. Furthermore, due to natural leaching from these reactive materials, contamination of the environment close to the deposits often occurs. The main problems are related to possible mobilizations of heavy metals and formation of acid mine drainages from the oxidation of sulphides. For this reason, the study of the pond geometry, the thickness of the mine tailings accumulated in it, as well as the presence or absence of inner water flows and the location of acid drainage leaks are all essential for a conclusive assessment of the environmental risk.

In the SW of the Iberian Peninsula, there are a large number of mine ponds related to the mining of the massive sulphide ores of the Iberian Pyrite Belt (IPB) (IGME 1986; Fig. 1). The 250 km-long Iberian Pyrite Belt is located in the South-Portuguese Zone, the southernmost terrane of the Variscan Belt of Iberia. Among other geological units, the belt includes the so-called volcanic sedimentary complex, Upper Devonian-Carboniferous in age, where massive sulphide bodies frequently occur. These are hosted by a complex felsic-mafic volcanic sequence interbedded with mudstone and several chemical sediments and are related to Variscan tectonics and hydrothermalism (Lunar *et al.* 2002; Almodóvar and Sáez 2004; Tornos 2006; and references cited therein).

The IPB hosts 82 inactive or working mines, as well as more than 38 ore showings of massive sulphides or stockworks, with a very high total tonnage/surface ratio of about 15 000–20 000 tonnes of massive sulphides per hectare of outcropping volcanic sedimentary complex. Despite their large size, most are pyrite-rich and only 11 deposits show important Cu–Zn–Pb contents (Tornos 2006). Many of the major ore deposits consist of several (two to six) individual massive sulphide lenses clustered in a small area of just a few square km, as occurs in the giant deposits of Neves Corvo, Aljustrel, Tharsis, Sotiel–Migollas, Rio Tinto and Aznalcóllar–Los Frailes. The intense mining activity in the district has produced a large number of mining waste deposits, most of them nowadays abandoned, which constitute an important environmental problem (Blanco *et al.* 2003; López *et al.* 2007; Pérez-López *et al.* 2007). In the case of mine ponds, they

* david.gomez@urjc.es

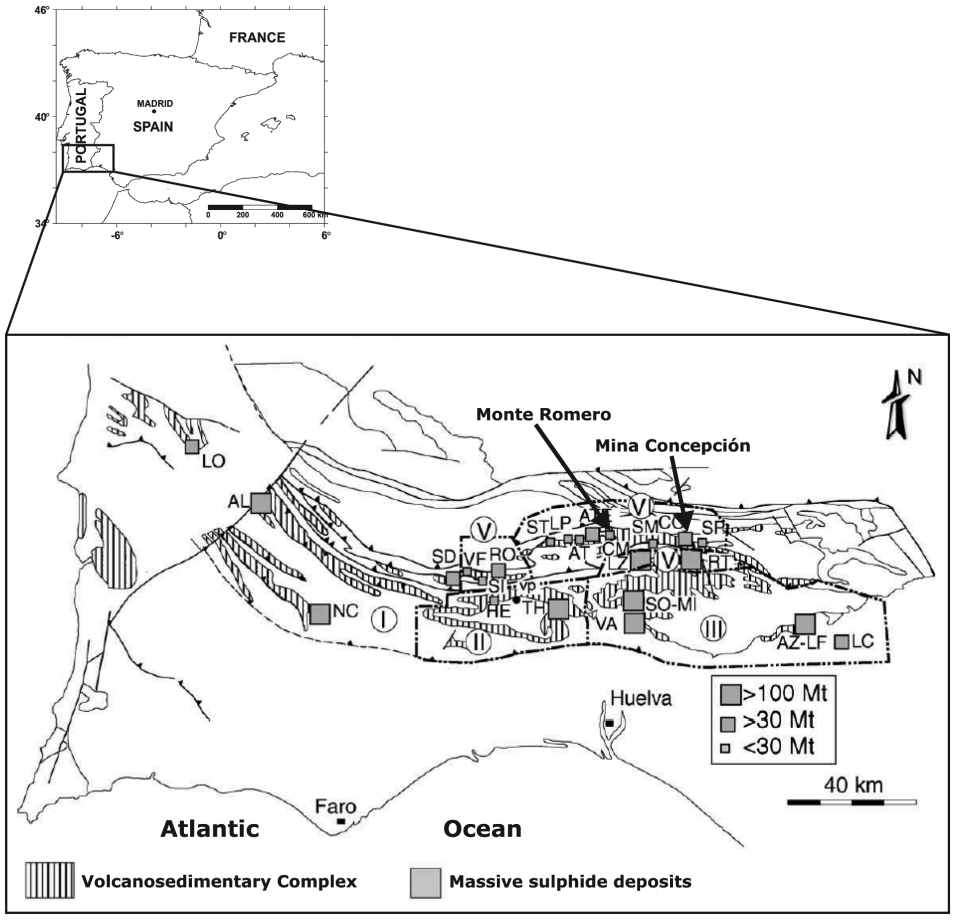

FIGURE 1
Geologic scheme with location of main massive sulphide exploitations in the Iberian Pyrite Belt (modified from Tornos 2006).

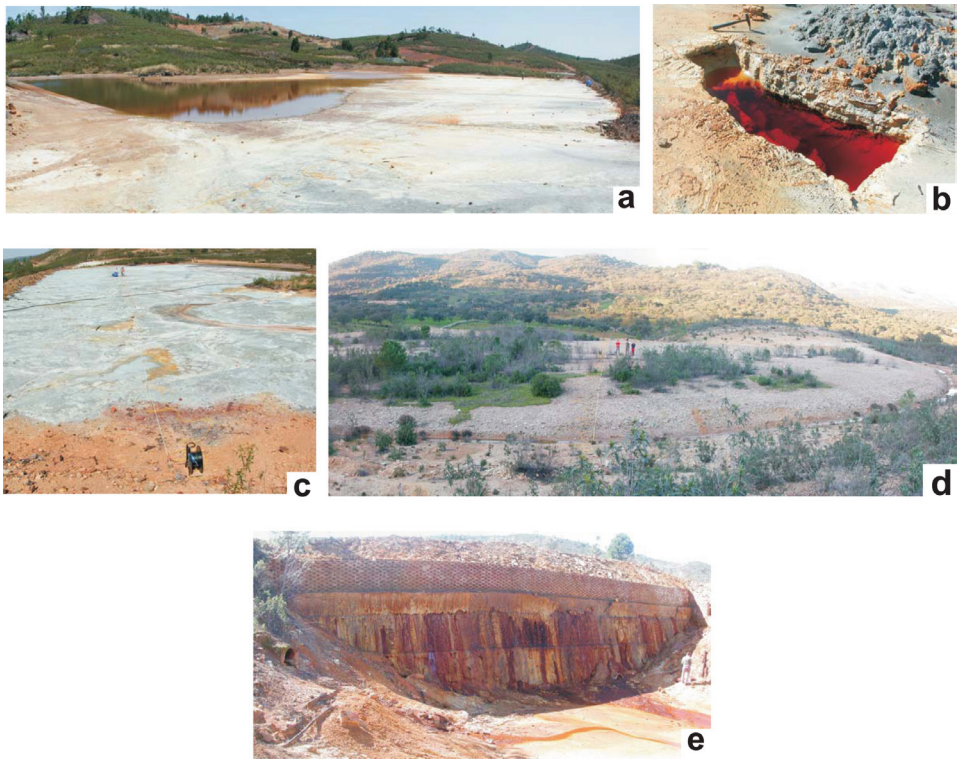

FIGURE 2
a) General view of the Monte Romero abandoned mine pond; b) small ditch showing the water level. Note the colour of the acid water caused by the iron content; c) electric longitudinal profile at the easternmost mine pond (profile 3); d) main view of the Mina Concepción abandoned mine pond; e) detail of the containment dam with acid water drainage.

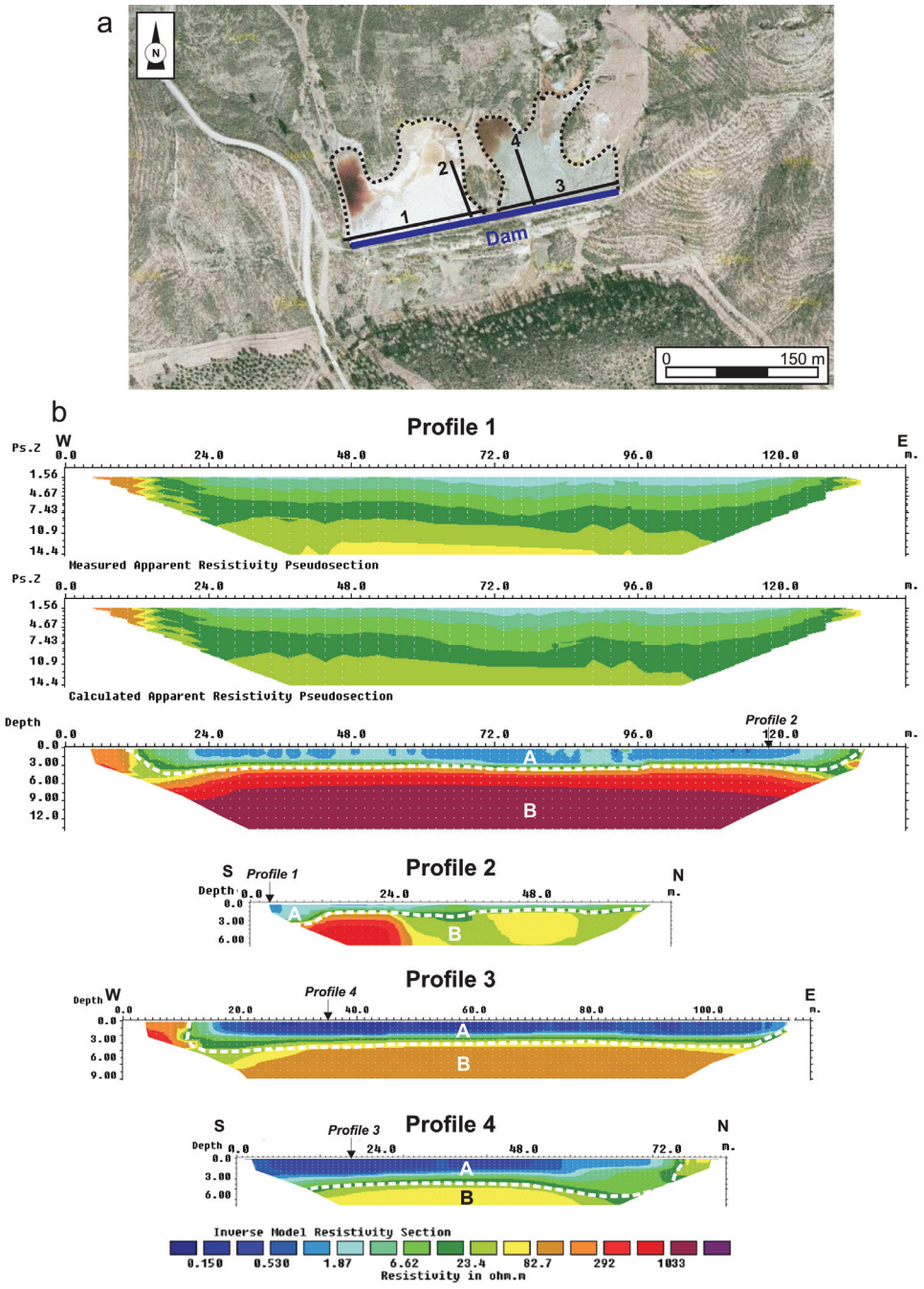

FIGURE 3

a) Location of ERT profiles in Monte Romero mine pond. The dotted line delineates the boundary of the ponds; b) ERT profiles showing the infilling materials and the geometry of the base of the mine pond. For profile 1, both measured and calculated apparent resistivity sections are shown, together with the inverted model section. For profiles 2, 3 and 4, only the inverted model is shown.

are constituted by fine-grained materials that represent a source of accumulation and subsequent emission of heavy metals, with formation of acid drainage by sulphide oxidation.

Mine ponds represent large volumes of materials derived from the metallurgical processes carried out for metal extraction. Classical treatments for base metal rich massive sulphide ores include crushing to fine fraction and further treatment in a flotation plant, where the metallic grains with no economic interest (e.g., pyrite, arsenopyrite) pass to the tailing of process and are subsequently transferred, as water-saturated material, to a decantation pond.

The deposits form a sedimentary sequence of centimetric beds, differentiated by compositional and/or grain size variations. Thus, they commonly display medium-to finegrained size and they include a significant amount of sulphides, either with no economic interest or not recovered due to deficient extractive technologies. These compositional and textural differences in the beds produce, in turn, a different geophysical behaviour, for

instance, in terms of transmission of an electrical current or conductivity. Therefore, the analysis of those variations in behaviour may allow identifying and locating the differences in the nature of material. In addition, the presence of water and variations in its content may be evaluated since the conductivity is strongly dependent of ionic species dissolved in pore water.

In the present work, a geophysical prospection technique (electrical resistivity tomography) is used to characterize two abandoned mine ponds related to sulphide extraction in the IPB: Monte Romero and Mina Concepción. The main goals of the study are: a) to establish their pond morphology and the thickness of deposits, b) to characterize their horizontal and vertical distributions of the materials and c) to identify the occurrence of internal water flows and potential acid drainage leaks.

DESCRIPTION OF THE MINE PONDS

The abandoned mine ponds are located in two different mine sites belonging to the Rio Tinto mine district (Huelva province): two ponds correspond to the Monte Romero mine site and another one to the Mina Concepción mine site (Fig. 1). All of them are the result of the piling up of medium-to-fine grained material, resulting from grinding and mineral processing.

The Monte Romero mine ponds (Fig. 2a–c) are located near the Cueva de la Mora village. These tailings lie over Carboniferous shales that represent the main lithology in the area. They are the final product of an abandoned mine exploitation of sphalerite and galena, exhibiting a siliceous composition with variable contents of pyrite (Blanco *et al.* 2003). The dimensions of both ponds are respectively 125 m × 80 m for the westernmost and 90 m × 70 m for the easternmost one, being divided by a small topographic escarpment (Fig. 3a). During the field survey, both mine ponds were flooded in its northernmost part and the water table in the westernmost pond was located at a maximum depth of 0.5 m, as observed in a small ditch. For these ponds, Blanco *et al.* (2003) described water table depths ranging from 0.5 m during the winter to about 3 m during the summer. Water is drained from the ponds to a small local creek (Monte Romero creek) by means of a plastic pipe.

The Mina Concepción restored mine pond is located on the SE of the Almonaster la Real municipal district, to the NW of the Minas de Rio Tinto town (Fig. 2d–e). It has 180 m × 60 m maximum dimensions, which correspond to a surface extension of ~10 000 m^2 and a volume around 30 000 m^3. The mine tailings, which are the result of the extraction and recovery of pyrite, have been deposited on volcanic lithologies (basic tuffs of Carboniferous age) on the slope of the Cerro de la Corta hill. It has a drainage system with an overflow channel, for the construction of which a watercourse had to be diverted. Drained waters from this pond run into the river Odiel.

The area affected by the Mina Concepción mine site was restored by the Environmental Council of the Junta de Andalucía (Consejería de Medio Ambiente 1997). In a first stage, the physical reclamation of the mine pond was carried out including the remediation of zones with pollutants contributions and in a second stage, the landscape integration of the mine pond was achieved, with its sealing and the replanting of 20 000 m^2 of ground. A ditch skirts around the perimeter of the mine pond, in order to facilitate the lateral drainage of meteoric waters and avoid their infiltration. Despite this, acid drainage comes from the mine pond through the dyke and drainage pipes, flowing down to a small stream running into the river Odiel. Overlying the mine tailing deposits, there is a layer of 30–50 cm of sandy clays with boulders. These detritic sediments are gravels and angular pebbles on the most superficial part, grading into sandy clays with boulders directly overlying the mine tailing deposits. The latter clearly showed oxidation signs on their first 5 cm. At present, vegetation cover does not exceed one fourth of the mine pond surface.

METHODOLOGY

Electrical resistivity tomography (ERT) is a geophysical prospecting technique designed for the investigation of areas of complex geology. Usually, the technique is carried out using a large number of electrodes, 24 or more, connected to a multi-core cable. A laptop microcomputer together with an electronic switching unit is used to automatically select the relevant four electrodes for each measurement. Since increasing separation between electrodes provides information from increasingly greater depths, the measured apparent resistivity can be inverted to provide a cross-section of true resistivity along the survey line.

The principal applications of this technique include (see for example Telford *et al.* 1990; Reynolds 1997; Šumanovac 2006): definition of aquifer boundary units, such as aquitards, bedrock, faults and fractures; the detection of voids (e.g., Gómez-Ortiz *et*

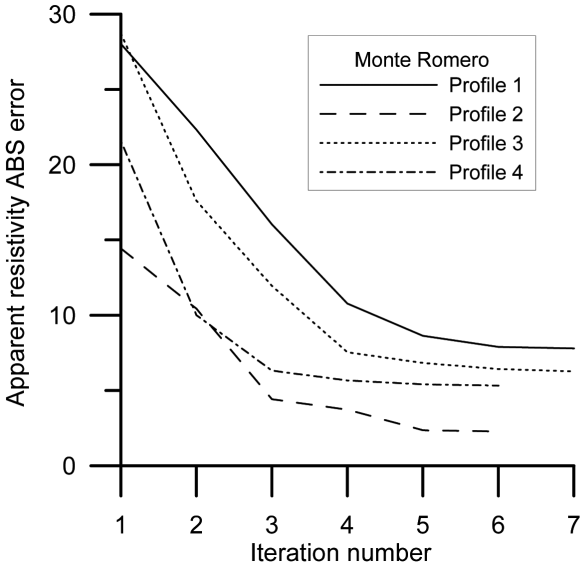

FIGURE 4
Plot of the change of apparent resistivity absolute error with iteration number for the ERT profiles at Monte Romero mine pond.

al. 2007); the mapping of saltwater intrusions into coastal aquifers; the identification of contaminated groundwater plumes; the detection of mineralized zones and, the exploration of sand and gravel resources, among others. Regarding the application of electrical and electromagnetic techniques to the characterization of mine waste deposits and related contamination, good examples can be found in Merkel (1972), Campbell and Fitterman (2000) and Buselli *et al.* (1998). ERT technique has mainly been used on waste piles (Yuval and Oldenburg 1996; Painter *et al.* 2000) or tailings dams (Niederleithinger and Kruschwitz 2005; Sjodahl *et al.* 2005), whereas few studies have focused on the internal structure of tailings ponds (e.g., Kuras *et al.* 2008; Zogala *et al.* 2008; Martínez-Pagán *et al.* 2009).

Several standard electrode arrays are available, with different horizontal and vertical resolution, penetration depth and signal-to-noise ratio (e.g., Sasaki 1992). Among them, the more frequent are the dipole-dipole, Wenner and Wenner-Schlumberger. In order to combine a good penetration depth, a reasonable vertical and horizontal resolution and a good signal-to-noise ratio, the Wenner-Schlumberger array has been chosen for this study. This array has been successfully used by other authors in similar studies (e.g., Martínez-Pagán *et al.* 2009).

A significant resistivity contrast exists between the bedrock of the mine ponds and their infilling material. This fact allows obtaining useful results in order to define the depth to the mine pond bottom and consequently, the geometry and thickness of the infilling material. Examples of characterization of mine pond geometry can be found in Martínez Pagán (2006), Aracil *et al.* (2006) and Faz Cano *et al.* (2006) among others.

A Syscal Junior Switch 48 equipment was used in this work. The length of the ERT profiles ranged from 47–235 m, with electrodes spaced between 1–5 m, respectively, obtaining an approximately penetration depth of 25 m (Bernard 2003). The field data include resistance measurements between various electrodes and related geometrical information. An apparent resistivity value is calculated using the resistance measurements and the geometry of the array. These data are plotted as a pseudosection, which is a plot of the distribution of the apparent resistivity values based on the geometry of the electrodes. Pseudosections are inconclusive, therefore they need to be inverted into sections of

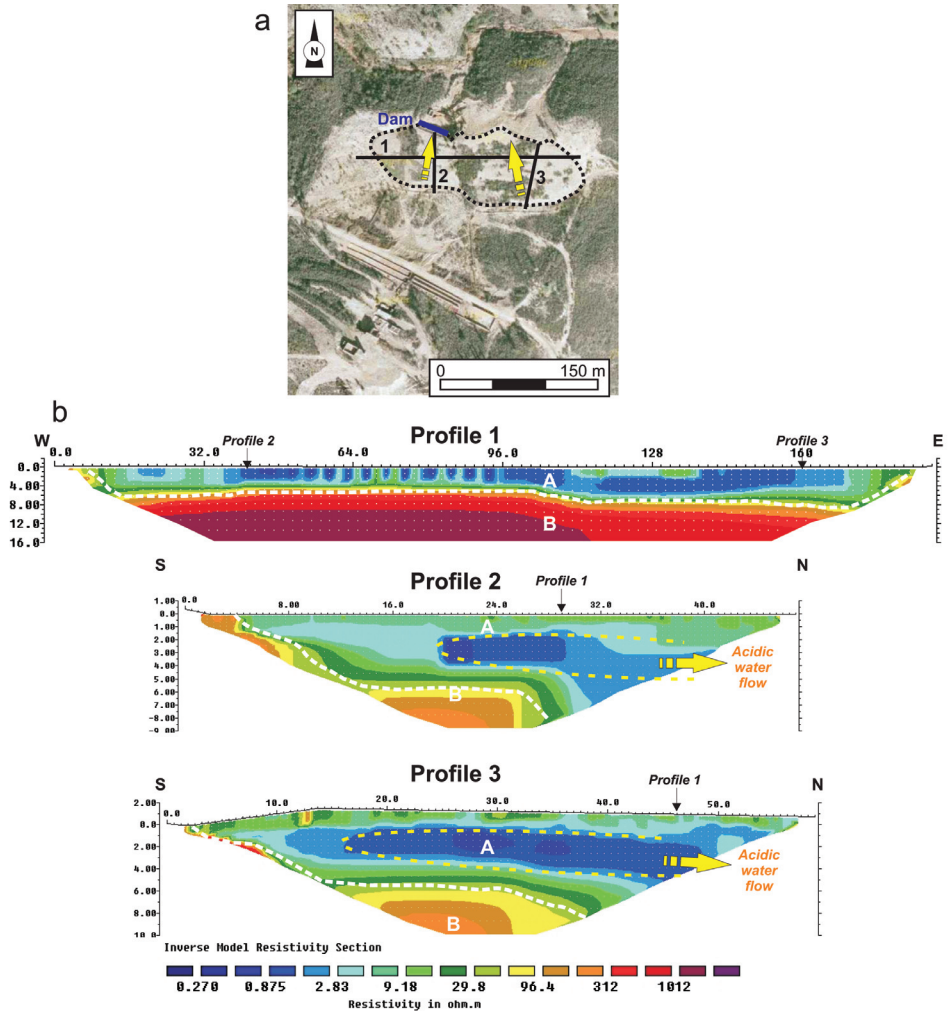

FIGURE 5
a) Location of ERT profiles in Mina Concepción mine pond. The dotted line delineates the boundary of the pond. Yellow arrows indicate the direction of the inferred acid water flow; b) ERT longitudinal and transverse profiles showing the infilling materials, the geometry of the base of the pond and the internal water flow.

true resistivity values and depths through a data inversion procedure that facilitates interpretation. In this study, inversion of resistivity data was performed using RES2DINV code (Loke and Barker 1995, 1996). For each data set, L1 norm was used for the data misfit and the inversion was carried out using the L1 norm (robust) for the model roughness filter (Loke *et al.* 2003). Robust inversion is more capable of handling sharp boundaries in the model and was used in all inversions, due to the expected large contrasts in electrical properties of the involved materials. The method uses a finite element scheme for solving the 2D forward problem and blocky inversion method for inverting the ERT data. RES2DINV generates the inverted resistivity image for each line. The quality of inversion result was checked by monitoring absolute error (e_{abs}) between the measured and predicted apparent resistivity given by,

$$e_{abs} = \sum_{i=1}^{N} \left[\frac{\left| \log(\rho_{a_{meas}}) - \log\left(\rho_{a_{calc}}\right) \right|}{N} \right], \quad (1)$$

where $\rho_{a_{meas}}$ and $\rho_{a_{calc}}$ are the measured and calculated apparent resistivity values at ith data point, respectively and N is the total number of data points.

The inverted section is then used to interpret the subsurface lithology. Data processing steps consist in removing bad data points, including the topography data along the profile.

It is a well-known fact (e.g., Loke 2004) that, if there are significant variations in the subsurface resistivity in a direction perpendicular to the survey line, this may cause distortions in the lower sections of the 2D obtained model. Several works (e.g., Dahlin and Loke 1997) have studied the sensitivity of different arrays to structures off the axis of a 2D survey line. From them, it can be concluded that dipole-dipole is the most sensitive array, whereas the Wenner array produces the smallest 3D effects. Taking this into account, the Wenner-Schlumberger array used in this study is not very sensitive to 3D effects and the distance from the profiles to features that are likely to introduce artefacts into the models (e.g., the embankment dams) is never shorter than 10 m. Therefore, we can deduce that, although the presence of 3D structures can potentially lead to larger errors during the inversion, they are not likely to be high enough to invalidate the results of this study.

RESULTS

Monte Romero mine ponds

Two symmetrical pairs of ERT profiles (one longitudinal, one transverse) were carried out at each of the Monte Romero mine ponds, in order to cover all available exposure (Fig. 3). Profile 1, longitudinal to the dyke in the westernmost pond, has a length of 141 m, an electrode spacing of 3 m and a maximum survey depth of 13.5 m. The absolute error during the inversion process, reached at the seventh inversion, was 7.8% (Fig. 4). In order to provide information about quality of inverse model, both measured and calculated apparent resistivity pseudosections have been provided for this profile together with the inverted section (Fig. 3b). However, for the sake of brevity, only the inverted sections have been plotted for the rest of the profiles. Two main units with very different resistivity values can be observed in the ERT plot (Fig. 3): an upper unit (unit A) extending from 12–135 m along the profile, with resistivity ranging from <1–25 Ωm and a lower one (unit B) with a resistivity ranging from 25 to >2000 Ωm. Unit A exhibits lateral boundaries at the surface with a steep dip at the surface that flatten as the infilling thickness increases. The base of this unit, slightly undulating, is located at 3 m depth.

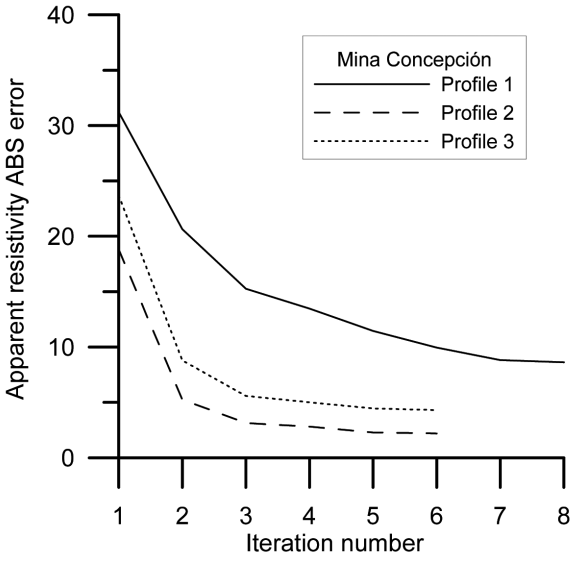

FIGURE 6
Plot of the change of apparent resistivity absolute error with iteration number for the ERT profiles at Mina Concepción mine pond.

Profile 2, transverse to the dyke, has a length of 70.5 m, with an electrode spacing of 1.5 m, reaching a maximum penetration depth of 7 m. The minimum absolute error during the inversion process was 2.3%, reached at the sixth iteration (Fig. 4). As in the previous profile, two different units can be distinguished (Fig. 3). The upper one (unit A) has low-resistivity values (<1–25 Ωm) and a thickness of 3.5 m near the dyke that diminishes to 1.5 m toward the north. The lower unit (unit B) shows two slightly different sectors: the first one, extending as far as 25 m distance and characterized by resistivity values higher than 88 Ωm and the second one, from 25 m onward, displaying resistivity values from 25–88 Ωm, probably indicating differences in the weathering degree of the shales.

In the easternmost pond, ERT profile 3 (longitudinal to the dyke) has a length of 117.5 m, with an electrode spacing of 1.25 m. The maximum penetration depth obtained is 10 m. The minimum absolute error during the inversion process was 6.3%, reached at the seventh iteration (Fig. 4). The resistivity values are, in general, lower than those obtained for the western pond. A 7 Ωm

contour level allows us to distinguish between two different units: an upper one (unit A) that exhibits the lowest resistivity values and a lower one (unit B) with resistivity values higher than 7 Ωm. The boundary between both units is located at 3.5 m mean depth, steeping towards the limits of the mine pond.

The length of transverse profile 4 is 82.25 m, with an electrode spacing of 1.75 m and a maximum penetration depth of 7.8 m. The absolute error obtained during the inversion process was 5.3% at the sixth iteration (Fig. 4). In this profile, the thickness of unit A decreases from 4 m near the dyke to 3 m far from it, steepening abruptly towards the end of the profile where this unit reaches the surface at a horizontal distance of 75 m from the beginning of the profile.

Mina Concepción mine pond

As in the case of Monte Romero, the dimensions at Mina Concepción allowed covering all its exposed area with three ERT profiles: one longitudinal and two transverse to the dyke (Fig. 5). Profile 1 (longitudinal) at this mine pond is 188 m long, with an electrode spacing of 4 m and a maximum depth of investigation of 16 m. The minimum absolute error during the inversion process was 8.6%, reached during the eighth iteration (Fig. 6). Similar to the previous examples, two different units can be identified. The upper one (unit A) is characterized by low-resistivity values (<0.2–30 Ωm), whereas the lower one (unit B) is represented by high-resistivity values (~1000 Ωm). Inside unit A, small areas with low (< 1 Ωm) resistivity values can be identified. Most of them are located between 40 and 116 m. A wider, more continuous area of low resistivity can also be recognized between 118–144 m of the profile. The thickness of unit A is 5 m at its western part (along the first 100 m of the profile) and 7 m at the eastern part. Opposite to this, unit B is very homogeneous and has high-resistivity values.

Profiles 2 and 3 are very similar and therefore, are jointly described. Their lengths are 47 m and 58.75 m, respectively, with an electrode spacing of 1 m (profile 2) and 1.25 m (profile 3). Maximum penetration depths vary from 9–10 m. Minimum absolute values obtained during the inversion process (Fig. 6) are 2.2% (6th iteration) and 4.3% (6th iteration). The maximum thickness of unit A is 7 m in profile 2 and 5 m in profile 3. In both cases, a step in the base of the pond is clearly visible, such as the greater infilling thicknesses found near to the dam. It is important to note that in both transverse profiles there are slightly elliptical areas with resistivity values <1 Ωm inside unit A.

INTERPRETATION OF ERT DATA

Geometry of the mine pond's base

The ERT profiles obtained in the different mine ponds show some similarities. Thus, two main units can be distinguished in all of them: the upper one (unit A) is characterized by lower resistivity values (<25 Ωm) whereas the lower one (unit B) always displays higher resistivity. The upper one has been interpreted as the silt and clay materials conforming the infilling of the mine pond, whereas the second one would represent the metamorphic and volcanic materials defining the base of the mine pond. The latter is supported by the obtained resistivity values in this unit, which range from 50 to more than 2000 Ωm, in good agreement with the average of published data for both weathered and fresh shales and tuffs (e.g., Reynolds 1997). However, typical mean resistivity values for medium-to fine-grained sediments (e.g., Reynolds 1997) range from 50–150 Ωm, i.e., they are higher than the ones obtained in this study for unit A. Nevertheless, it must be taken into account that the infillings of the different ponds are all water saturated and they contain a great abundance of different types of sulphides all showing, as is common, highly variable and very low-resistivity values (e.g., Reynolds 1997 established that the resistivity value of pyrite ranges from 2.9 10^{-5} to 1.5 Ωm whereas that for galena ranges from 3 10^{-5} to 300 Ωm). Thus, both factors satisfactorily justify the measured decrease of resistivity values in the infillings of the different mine ponds to values lower than 1 Ωm (profile 1, Monte Romero westernmost pond; longitudinal profile at Mina Concepción, see Figs 3 and 5).

The arrangement in two orthogonal directions of ERT profiles

TABLE 1

Parameters measured in water samples from Mina Concepción water (MCW) drainage in February 2007. EC: electrical conductivity; TDS: total dissolved solids; MCW-1 = water leaking through the dyke wall; MCW-2 = basal drainage; MCW-3 = lateral drainage; MCW-4 = surface of deep ochre red puddle; MCW-5 = bottom of deep ochre red puddle

	Physico-chemical parameters				**Composition** (μg/l)				
Sample	**pH**	**EC** (μS/cm)	**Eh** (mV)	**TDS** (ppm)	**As**	**Co**	**Cu**	**Pb**	**Zn**
MCW-1	2.20	16,780	418.0	8,348	>2000	>2000	>2000	44.1	>2500
MCW-2	2.55	1,059	543.8	530	1.1	134	>2000	66.8	>2500
MCW-3	2.25	4,361	602.6	2,178	5	940	>2000	59.3	>2500
MCW-4	2.15	8,297	628.0	4,153	1350	>2000	>2000	18.1	>2500
MCW-5	2.00	10,580	636.3	5,290	>2000	>2000	>2000	0.3	>2500

carried out for both the Monte Romero and Mina Concepción mine ponds, has allowed us obtaining the geometry of the pond's base. In general, it can be defined as a trough with a flat bottom surface and steeply dipping lateral boundaries. The thickness reaches its maximum near the pond's dam whereas it diminishes progressively further from it (Figs 3 and 5). However, important geometry variations as steps have been identified at the bottom of Mina Concepción pond, causing in turn variations in the infilling thicknesses. The mine ponds with a more homogeneous thickness are the ones from Monte Romero, with mean values of 3–3.5 m for both ponds. Regarding Mina Concepción, a step in the base at its central part produces a variation of thickness from 5–7 m.

Comparable results have also been obtained by different authors in waste piles and similar mine ponds using both ERT and electromagnetic methods. Yuval and Oldenburg (1996), Painter *et al.* (2000), Kuras *et al.* (2008) and Zogala *et al.* (2008) obtained information about the depth to the base of the pond as well as internal structure of the deposits. They found that the resitivity values for the infilling materials range from 6–25 Ωm, which is in good agreement with the results of this work. The resistivity values obtained are similar to those obtained by different authors, e.g., Martínez-Pagán *et al.* (2009) and Faz-Cano *et al.* (2006) described, for similar abandoned sulphide mine ponds located in La Unión (Murcia, Spain), resistivity values of <8 Ωm for fine grained tailings and >150 Ωm for bedrock (composed by Paleozoic schists and quartzites).

Acid water flow

The survey carried out at the two Monte Romero mine ponds shows that most of its unit A in both, interpreted as the pond infilling, shows resistivity values lower than 2 Ωm (Fig. 3). These low values, as already mentioned, correspond to water-saturated silt and clay materials with abundance of sulphides, mainly pyrite. Pyrite crystals are clearly visible in hand specimens, so its presence is corroborated by *in situ* observations. Moreover, the existence of a small trench close to the longitudinal profile in the western pond, allowed us identifying the presence of the water table at a depth of 0.5 m. In addition to this, unit B, interpreted as related to the Carboniferous shales that constitute the base of the mine ponds, exhibits very high and homogeneous resistivity values. This fact seems to corroborate that no acid water drainage occurs along the base of the pond.

ERT profiles carried out at Mina Concepción have revealed the occurrence of areas with resistivity values <1 Ωm (Fig. 5). The geometry of these zones is slightly elliptical and elongated. Their upper part corresponds to the inflow of surface water into the pond, whereas their lower part is located close to the old dam that defines the edge of the pond. Observations made during the field survey have corroborated the existence of an important leakage of acid water through the walls of the dam. Physico-chemical parameters and major ion concentrations obtained for the water leaking through the walls of the dam are both presented in Table 1. As can be seen, pH ranges from 2.00–2.55 confirming the acid character of the water. Electrical conductivity values range from 1,000 to more than 16 000 μS/cm, in good agreement with the low-resistivity values obtained in the inverse models. The high (up to 8,000 ppm) TDS and Eh (up to 636 mV) values confirm the fact that the water samples have an oxidizing nature as well as a high content of dissolved ions. In particular, the highest ion concentrations correspond to Zn, As, Co and Cu. According to this, the elliptical low-resistivity areas are interpreted as due to flow of meteoric waters entering into the mine pond, their pH being progressively lowered as the water moves towards the dam. The acidification process results from oxidization of pyrite contained in the infilling materials. This internal water flow would result in the leakage of acid water through the dam observed in the field, provoking a contaminant spill to the Odiel River and therefore an important environmental problem. However, it must be mentioned that the low-resistivity values (<1 Ωm) are confined to the interior of the mine pond, whereas the resistivity values of the lower unit are higher and homogeneous and so it is possible to infer that it is unlikely that acid flow occurs through the base of the restored mine pond.

In a similar way, different authors have used electrical methods to delineate acid mine drainage in groundwater related to sulphur tailings dams (e.g., Merkel 1972; Yuval and Oldenburg 1996; Buselli *et al.* 1998; Buselli and Lu 2001). These authors described typical resistivity values associated to the presence of acid plumes in a range from ~1–25 Ωm, depending on the pH and total dissolved solids (TDS) values of the acid waters. Those resistivity values agree well with the ones (generally <2 Ωm) obtained for both Monte Romero and Mina Concepción mine sites, where there is field evidence of acid mine drainage.

CONCLUSIONS

- The ERT technique constitutes a valuable method to obtain reliable information about the internal structure of abandoned mine ponds.
- ERT data have allowed us to determine accurately the geometry of the base of the mine ponds as well as the thickness of their infilling materials. This is due to the high-resistivity contrast existing between the fine-grained materials that constitute the infilling and the metamorphic and volcanic rocks that form the base of the pond.
- The differences in resistivity values obtained in the silt-clay materials of the infilling have provided useful information about heterogeneities in the pond and the existence of internal acid water flows. Low-resistivity areas (<1 Ωm) define the occurrence of the latter within all of the studied ponds, also allowing us to identify the recharge and discharge areas in the case of Mina Concepción. The materials that constitute the base of the studied mine ponds are characterized by high and homogeneous resistivity values. This is due to a good isolation of the mine ponds boundaries and the absence of acid water leakage through the substrate. The only leakage detected occurs through a badly preserved dyke at Mina Concepción

mine pond that is clearly identified as much in the ERT profiles as directly in the field.

In summary, ERT technique has proven to be a useful tool to characterize the structure of mine ponds which constitute important volumes of mine waste disposal. The use of this non-destructive geophysical technique allows evaluating the environmental problems associated with the abandoned mine ponds and, in a later phase, to proceed with the remediation design. At a monitoring stage, once a mine pond has been restored, this technique is a very useful inspection tool in order to check the efficiency of the remediation measures applied (e.g., degree of isolation of the pond).

ACKNOWLEDGEMENTS

This study was supported by Project URJC-RNT-063-1 with financial support from the Comunidad de Madrid and the Universidad Rey Juan Carlos. We wish to thank two anonymous reviewers and the Editor for their constructive comments, which have greatly contributed to improve the manuscript.

REFERENCES

Almodóvar G.R. and Sáez R. 2004. Los sulfuros masivos de la Faja Pirítica Ibérica. In: *Geología de España* (ed. J.A. Vera), pp. 207–209. SGE-IGME, Madrid.

Aracil E., Porres J.A., Faz A., Martínez-Pagán P., Maruri U. and Vallés J. 2006. Balsas mineras abondonadas y balsas de purines: dos problemas medioambientales abordables mediante tomografía eléctra. III Congreso de Ingeniería Civil, Territorio y Medio Ambiente. www.ubu.es/investig/aulavirtual/ Posters/Balsas.pdf.

Bernard J. 2003. Short note on the depth of investigation of electrical methods. IRIS Instruments, Orleans, France.

Blanco A., Lloret A., Carrera J., Saaltink M.W., Acero P., Ayora C. and Nieto J.M. 2003. Monitorización del movimiento del agua a través de una balsa de lodos residuales mineros en la Faja Pirítica Ibérica (SO de la Península Ibérica). Jornadas Luso-Españolas sobre Aguas Subterráneas en el Sur de la Península Ibérica, Faro, Portugal, Expanded Abstracts, 1–10.

Buselli G., Hwang H.S. and Lu K. 1998. Minesite groundwater contamination mapping. *Exploration Geophysics* **29**, 296–300.

Buselli G. and Lu K. 2001. Groundwater contamination monitoring with multichannel electrical and electromagnetic methods. *Journal of Applied Geophysics* **48**, 11–23.

Campbell D.L. and Fitterman D.V. 2000. Geoelectrical methods for investigating mine dumps. *5th International Conference on Acid Rock Drainage (ICARD2000)*, Society for Mining, Metallurgy, and Exploration, Inc., Denver, Colorado, 1513–1523.

Consejería de Medio Ambiente 1997. *Medio Ambiente en Andalucía. Informe 1996*. Junta de Andalucía, Sevilla.

Dahlin T. and Loke M.H. 1997. Quasi-3D resistivity imaging-mapping of three dimensional structures using two dimensional DC resistivity techniques. *Proceedings of the 3rd Meeting of the Environmental and Engineering Geophysical Society*, 143–146.

Faz-Cano A., Martínez-Pagán P., Aracil E. and Maruri U. 2006. Aplicación de la tomografía eléctrica al estudio de los depósitos de estériles mineros "El Lirio" y "Brunita" (Murcia). In: *Los residuos minero-metalúrgicos en el medio ambiente* (eds R. Rodríguez and A. García Cortés), pp. 89–110. IGME, Madrid.

Gómez-Ortiz D., Martín-Velázquez S., Martín-Crespo T., Márquez A., Lillo J., López I. *et al*. 2007. Joint application of ground penetrating radar and electrical resistivity imaging to investigate volcanic materials and structures in Tenerife (Canary Islands, Spain). *Journal of Applied Geophysics* **62**, 287–300.

IGME 1986. *Inventario nacional de balsas y escombreras*. Madrid.

Kuras O., Banks V., Palumbo-Roe B. and Klinck B. 2008. Geophysical imaging of a tailings lagoon at an abandoned lead-zinc mine in the central wales orefield, UK. Near Surface meeting, Krakow, Poland, Expanded Abstracts.

Loke M.H. 2004. *Tutorial: 2-D and 3-D Electrical Imaging Surveys*. Geotomo Software, Malaysia.

Loke M.H., Acworth I. and Dahlin T. 2003. A comparison of smooth and blocky inversion methods in 2D electrical imaging surveys. *Exploration Geophysics* **34**, 182–187.

Loke M.H. and Barker R.D. 1995. Least-square deconvolution of apparent resistivity pseudo-sections. *Geophysics* **60**, 499–523.

Loke M.H. and Barker R.D. 1996. Rapid least-squares inversion of apparent resistivity pseudosections by a quasi-Newton method. *Geophysical Prospecting* **44**, 131–152.

López M., González I. and Romero A. 2007. Trace elements contamination of agricultural soils affected by sulphide exploitation (Iberian Pyrite Belt, SW Spain). *Environmental Geology* **54**, 805–818. doi:10.1007/s00254-007-0864-x

Lunar R., Moreno T., Lombardero M., Regueiro M., López-Vera F., Martínez del Olmo W. *et al*. 2002. Economic and environmental geology. In: *The Geology of Spain* (eds W. Gibbons and M.T. Moreno), pp. 473–510. Geological Society of London.

Martínez Pagán P. 2006. *Aplicación de diferentes técnicas no destructivas de prospección geofísica a problemas relacionados con contaminación ambiental producida por diferentes actividades antrópicas en la Región de Murcia*. PhD thesis, Universidad Politécnica de Cartagena.

Martínez-Pagán P., Faz-Cano A., Aracil E. and Arocena J.M. (2009). Electrical resistivity tomography revealed the spatial chemical properties of mine tailings ponds in the Sierra Minera (SE Spain). *Journal of Environmental & Engineering Geophysics* **14**, 63–76.

Merkel R.H. 1972. The use of resistivity techniques to delineate acid mine drainage in ground water. *Ground Water* **10**, 38–42.

Niederleithinger E. and Kruschwitz S. 2005. Multi-channel spectral induced polarization (SIP) measurements on tailings dams. Near Surface meeting, Palermo, Italy, Expanded Abstracts.

Painter M.A., Laverty B., Stoertz M.W. and Green D.H. 2000. Resistivity imaging of a partially reclaimed coal tailings pile. In: *Symposium on the Application of Geophysics to Engineering and Environmental Problems* (eds M.H. Powers, L. Cramer and I. Abou-Bakr), pp. 679–688. EEGS.

Pérez-López R., Cama J., Nieto J.M. and Ayora C. 2007. The iron-coating role on the oxidation kinetics of a pyritic sludge doped with fly ash. *Geochimica et Cosmochimica Acta* **71**, 1921–1934. doi:10.1016/j.gca.2007.01.019

Reynolds J.M. 1997. *An Introduction to Applied and Environmental Geophysics*. John Wiley and Sons.

Sasaki Y. 1992. Resolution of resistivity tomography inferred from numerical simulation. *Geophysical Prospecting* **40**, 453–464.

Sjodahl P., Dahlin T. and Johansson S. 2005. Using resistivity measurements for dam safety evaluation at Enemossen tailings dam in southern Sweden. *Environmental Geology* **49**, 267–273.

Šumanovac F. 2006. Mapping of thin sandy aquifers by using high resolution reflection seismics and 2-D electrical tomography. *Journal of Applied Geophysics* **58**, 144–157.

Telford W.M., Geldart L.P., Sheriff R.E. and Keys D.A. 1990. *Applied Geophysics*. Cambridge University Press.

Tornos F. 2006. Environment of formation and styles of volcanogenic massive sulfides: The Iberian Pyrite Belt. *Ore Geology Reviews* **28**, 259–307.

Yuval D. and Oldenburg D.W. 1996. DC resistivity and IP methods in acid mine drainage problems: results from the Copper Cliff mine tailings impoundments. *Journal of Applied Geophysics* **34**, 187–198.

Zogala B., Pierwola J., Dubiel R. and Cabala J. 2008. Geoelectrical survey in the area of a long-lasting Zn-Pb waste storage. Near Surface meeting, Krakow, Poland, Expanded Abstracts.